Movement tracking of the carotid artery with 4D ultrasound imaging

Anny Eriksson-Bernholtz

2019

Master's Thesis in Biomedical Engineering

Supervisor: Tobias Erlöv
Co-supervisor: Magnus Cinthio
Examiner: Hans W. Persson

LUND UNIVERSITY

LTH

FACULTY OF ENGINEERING

Department of Biomedical Engineering

Abstract

The leading cause of death in the world is cardiovascular diseases. Scientific discoveries have been made that correlate the movement of the arterial walls and blood flow patterns with cardiovascular diseases. These movements have been studied with ultrasound 2D imaging. From 2D movement tracking it is observed that the arterial wall moves in two directions, radially and longitudinally, and research has made connections from the patterns of movement to cardiovascular diseases. Blood flow patterns have been studied in 3D, with Doppler ultrasound and 3D MRI, and spherical blood flow patterns have been distinguished. This thesis is a first attempt to study the arterial wall movement of the common carotid artery with the use of 4D ultrasound imaging. To do this 4D ultrasound images were constructed by acquiring 2D motion images of the common carotid artery of three healthy volunteers, triggered with the use of ECG signals. These images were put through a 3D shift phase tracking algorithm developed for this thesis, using a program called MATLAB. To view the motion tracking of the arterial wall, a three-dimensional segmentation was created manually using 2D-slices. Applying the motion tracking to the coordinates of the segmented shape, a motion 3D image could be seen. It was not possible to draw any conclusions from this moving shape, so two other methods were used for validation of the 3D tracking algorithm. The first method used 2D slices, plotting a moving segmented slice on top of the corresponding ultrasound 2D image slice, to observe if the movement followed the original image. The second method compared the results in movement plots, plotting the 2D movement both radially and longitudinally and comparing this with an existing validated 2D shift phase tracking method. The results showed that the 3D motion tracking worked better in the radial direction than in the longitudinal direction, however neither results were completely correct. With many possible error sources, this method still seems promising, and one main issue is the resolution of the images, which needs to be increased for better results.

Populärvetenskaplig sammanfattning

Rörelsedetektering av halspulsådern med ultraljudsbilder i 4D

I denna studie har ett första försök till att mäta rörelsen i blodkärlsväggen hos halspulsådern med fyrdimensionella ultraljudsbilder gjorts. Mätningar av rörelsen i blodkärlsväggarna kan ge värdefull information om eventuella hjärt- och kärlsjukdomar.

Hjärt- och kärlsjukdomar är orsaken till 30 % av världens alla dödsfall. År 2030 förväntas så många som 23.6 miljoner människor att dö av hjärt- och kärlsjukdomar och man förutspår även att detta kommer att fortsätta vara den huvudsakliga dödsorsaken i världen. Det är därför viktigt att skapa sig en så bred bild som möjligt av sjukdomsförloppen för att kunna spara resurser, motverka sjukdomar och motverka dödsfall.

Upptäckter inom vetenskapen har gjort att man har kunnat dra paralleller mellan hur blodkärlsväggar rör sig och hjärt- och kärlsjukdomar. Man har också kunnat dra paralleller med hur blodet i ett blodkärl flödar och hjärt- och kärlsjukdomar. En speciell rörelse som upptäckts är att blodet flödar i en spiralrörelse. Väggen i ett blodkärl sägs röra sig på två olika sätt. Det ena är att hela blodkärlet expanderar radiellt (diametern av blodkärlet förändras) under tiden av en hjärtcykel. Detta är det vanligaste sättet att titta på blodkärlets rörelser på. Den andra rörelsen sker längs med blodkärlets riktning, där två av de tre lagerna i blodkärlsväggen förflyttar sig under hjärtcykeln. Det finns mycket kunskap om hur radiella rörelser hänger ihop med kardiovaskulära sjukdomar, men inte så mycket om longitudinella rörelser än.

Mätningar av blodkärlsrörelser i 2D går att göra med ultraljudsmaskiner. Det finns flera fördelar med ultraljudsdiagnostik som inkluderar att de kan göras icke-invasivt och med låga kostnader. Detta jämförelsevis med andra medicinska bildtagningsmetoder så som magnetisk resonanstomografi och CT röntgen. Det är därför av stort intresse att fortsätta utveckla metoder för ultraljudsmätningar i samband med hjärt- och kärlsjukdomar

för att kunna dra nya slutsatser och lära oss mer om hur blodkärlets rörelse är kopplat till olika hjärt- och kärlsjukdomar.

De flesta medicinska mätningar sker i 2D, vilket begränsar kunskapen om hur dessa olika rörelser korrelerar. Nu på senare tid har man börjat alltmer med 3D-bilder för att kunna tydligare se hur organen och vävnaden i kroppen ser ut. Däremot så är det ingen som försökt mäta blodkärlsväggens rörelser i 3D, och då heller sett om det finns något samband mellan den longitudinella rörelsen, den radiella rörelsen och det spiralformade blodflödet.

I detta examensarbete har ett program skapats för att analysera rörelser i 3D med användning av 4D-ultraljudsbilder (3D-filmer). Ultraljudsmätningar har gjorts på halspulsådern för att se om man kan detektera eventuella 3D-rörelser. Programvaran som användes var MATLAB, där rörelsedetekteringsalgoritmen skapades, i detta första försök av att mäta rörelsen i halspulsådern i 3D. Resultaten jämfördes med 2D-rörelsedetektering framtagen av en tidigare beprövad algoritm. Slutsatsen visar att det är möjligt att göra rörelsemätningar med 4D-ultraljudsbilder. En svårighet med att arbeta med 4D-filer är att de är väldigt stora och kräver mycket processorkraft och tid för att genomföra beräkningar på. I detta projekt var även upplösningen hos 4D-filerna ett problem. Ökad upplösning spelar stor roll för att kunna få bättre resultat i framtiden. För att kunna använda denna metoden diagnostiska sammanhang behövs fortsatt utveckling, då resultaten ej var perfekta, även om de var lovande.

Table of Contents

List of Figures

List of Tables

Chapter 1
Introduction

This chapter will first present the scientific background of this thesis. Secondly, previous research publicized within the department of Biomedical Engineering at Lund University, which preludes this thesis will be presented. Lastly the aim for this thesis will be given.

1.1 Background

Cardiovascular diseases are currently the leading cause of death in the world [1]. If we could gain more knowledge about the cardiovascular system and related diseases, this information could be used to prevent sickness, suffering, deaths and loss of resources. Research aiming for increasing the understanding of the cardiovascular diseases, i.e. how to detect, treat and prevent the cardiovascular diseases is continuously in progress. One of these important research areas is within the non-invasive diagnostic tools for detection of early stages of vascular diseases. There is ongoing research on the motion of the blood vessel walls and how this can be used for future pathological diagnostics [2]-[7]. There has been extensive research on how the arterial walls expand in the radial direction (motion parallel to the diameter of the arterial wall), but not until more recently has there been more research on how the walls move longitudinally (motion parallel to the arterial wall) [2]. The movement of the arterial walls have been studied and correlations between health and other physical factors have been found to affect wall motion and elasticity. Other research has studied and shown how the blood flows in the arteries. Studies have found that blood flows in certain patterns correlating to the physical state of the arteries, with the help of Doppler ultrasound and 4D MRI [8]. Some of these patterns are helix-shaped, which means the blood flows in a spiral motion. With the current knowledge of blood flow patterns, radial arterial wall movement and longitudinal arterial wall movement, there is an interest to see if these anatomical physical patterns correlate. With 3D motion tracking it might

be possible to see if the spiral pattern of the blood flow correlates to the movement of the arterial walls, and if there exists a spiral motion pattern in the arterial wall as well. No one has previously tried to measure the arterial wall motion in 4D ultrasound images, and these questions remain unanswered. Therefore it is of interest to try and view and use motion tracking on 4D ultrasound images of the arterial wall.

Ultrasound is a typically inexpensive and feasible non-invasive diagnostic tool and is already used in many applications within health care. If possible, the use of ultrasound for pathological diagnosis would be preferable to other imaging techniques, due to the easy accessibility and low cost. Ultrasound is easy to use when looking at the softer tissue of the body, for example blood, heart, bladder, fetus etc. Therefore it is of extra interest to perform motion tracking on the arteries with the use of non-invasive ultrasound.

1.2 Previous research at Lund University

This thesis is a continuation of previous research on arterial wall movement with ultrasound imaging, done by a collaboration of the department of Biomedical Engineering and the Department of Translational Medicine, both departments of Lund University, Lund, Sweden. In their article, Persson et al. (2003) presented a new method for simultaneous measurement of both longitudinal and radial arterial wall movement. It also states that longitudinal wall movement could have significant meaning for physiological knowledge of the arterial wall, and that this is a relatively unexplored area. Cinthio et al. (2006) researched the longitudinal movement of the arterial wall and how the longitudinal movement creates shear strain within the arterial wall [4]. Here they found that it is mainly the intima-media complex that moves and the pattern of the longitudinal wall motion is probably health and age related, and that it is different even for healthy individuals. To further study how the longitudinal arterial wall motion changes due to physical factors, studies of the effects of adrenaline and other catecholamines on porcine were done [5] [6], with the conclusion that an increase in longitudinal movement in the common carotid artery is not necessarily affected by wall shear stress. The wall shear stress is a measurement of the affect of the force the blood has on the wall it flows over. The department has also researched and published methods for measuring the diameter change in the arterial wall and developed a new motion tracking algorithm.

1.3 Aim

The overall aim of this thesis is to develop a method for movement tracking of the carotid artery using 4D ultrasound images. To do this, the program MATLAB (The Mathworks Inc., Natick, MA) is used. A graphic user interface is created in MATLAB to read the data and to display results. 4D ultrasound images are 3D films, using each still 3D image and comparing it to the next for a movement analysis of the common carotid artery.

Since this is a pilot study, the specific aims changed throughout this thesis. The specific milestones set in the thesis are seen below.

- Create a GUI (graphical user interface) in MATLAB for displaying 2D ultrasound images.
- Developing supervisor Tobias Erlöv's motion tracking code from 2D to 3D images [9].
- Sampling data (3D films of the common carotid artery).
- Further development of GUI for manual segmentation and 3D viewing.
- Applying data to motion tracking.
- View and compare results.

Chapter 2
Theory

This chapter will start by explaining the physics behind ultrasound imaging. Ultrasound imaging is a combination of using the physics of ultrasound waves and the techniques for creating images with the use of these waves. Then a brief introduction to the cardiovascular system and how we can monitor the signals of the heart is given. We will also dig further into the movement of arterial walls and how this correlates to pathological diagnosis. Lastly, some different methods of motion tracking will be presented.

2.1 Ultrasound

Ultrasound waves are sound waves with a frequency of 20 kHz and above. This high frequency sound is inaudible for human ears, while other animals such as bats and dolphins use those high frequency sound waves. The inspiration for using ultrasound in human made applications are bats [10]. Sound waves are mechanical vibrations that travel through a medium. As with all physical waves, ultrasound waves reflect at the change of a medium and echoes back. This echo of ultrasound waves is the basis for ultrasound imaging. Ultrasound diagnostics is a non-invasive tool to observe and diagnose soft tissue in the human body. The first attempts of using ultrasound as a medical diagnostic tool was in the early 1900s, and in the year of 1949 it was for the first time used to be able to locate gallstones and breast masses. In the early 1950s the first 2D image was produced, and in the 1980s color Doppler was introduced into the ultrasound imaging. As with all technology, there is constant progress; resolution has increased over the years and we have since the beginning of the century started to experiment and use 3D and 4D ultrasound imaging [10].

Unlike electromagnetic waves, sound waves cannot travel in vacuum; they must travel through matter. The propagation of an ultrasound wave is a transfer of energy through a medium. A sound wave starts in a physical medium as a pressure change, then propagates as continuous pressure

change through particle displacement with regions of compression and rarefaction, see Figure 2.1.

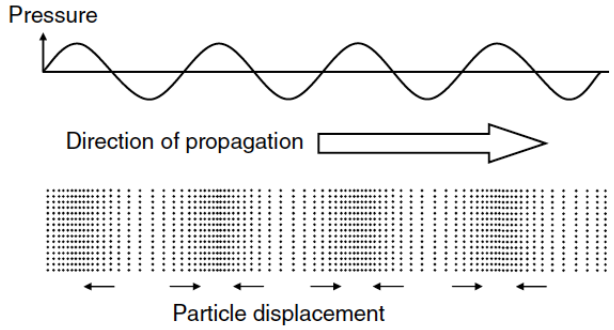

Figure 2.1: Illustration of how a longitudinal wave propagates, showing the pressure changes of the particles in combination with the particle displacement. From [11].

As all types of mechanical waves, sound waves travel with different speed depending on the properties of the transporting medium. The speed of propagation is determined by the stiffness and density of a medium. In a material with high density and low stiffness, the speed of sound will be low, and in a material with a low density and high stiffness the speed of sound will be high. In a medium with high density the particles are more compact, and with less vacuum the pressure changes will propagate more quickly than if they were further apart. Table 2.1 shows the speed of sound for different medium and tissue which are commonly used in medical ultrasound.

Table 2.1: The speed of sound in different medium. Data from [12].

Type of medium	Speed, c (m/s)
Air	343
Water	1480
Blood	1575
Liver	1590
Fat	1450
Bone	2800-4080
Kidney	1570

To explain the nature of a wave, three physical properties are used: the frequency, wavelength and propagation speed. These three physical properties are related according to (2.1), where λ is the wavelength, c is the

speed of the wave (propagation speed) and f is the frequency of the wave, i.e.

$$\lambda = c/f. \tag{2.1}$$

As seen in (2.1), the propagation speed of sound in the medium affects which wavelength the frequency of the wave will have.

Another physical property of a wave is the phase. The phase is measured in degrees, where a full cycle is 360° and marks the return to the original state. Sound waves passing through a medium move the particles of the medium, pushing the particles to and from their resting place in an oscillating pattern. The phase describes how far from the original state the particles of a medium are displaced. Two waves can have the same amplitude, frequency and wavelength, but have different phases. The phase is an important physical property, due to the ability of waves adding together through interference. If the phase is the opposite, the two waves will cancel each other through superposition. If they have the same phase they will add together and superimpose as one sound wave with twice the amplitude.

Attenuation

An ultrasound wave experiences loss of amplitude and intensity as it travels through a medium. The decline of amplitude occurs gradually; its loss can be seen as an exponential curve. This effect of loss of amplitude is called attenuation. The decrease of wave intensity over each unit of distance occurs with the same constant fraction for a specific medium and frequency; therefore it becomes an exponential curve of reduction in intensity. Attenuation occurs due to several different physical features of the sound wave. These are scattering, divergence, reflection, diffraction and absorption. All of these features behave differently in different medium and are also dependent on the frequency of the wave. Out of the different attenuation causes, absorption is the most important when it comes to ultrasound imaging. Absorption is when the intensity and amplitude of the sound wave decrease due to the surrounding medium absorbing the energy and converting the energy into heat. This effect is usually much larger than that of the other attenuation effects, since sound waves are easily converted into energy in human tissue.

In human tissue, the attenuation of ultrasound waves is dependent on the frequency of the wave. The attenuation effect increases with increased frequency. With a higher frequency the ultrasound wave will be absorbed into the tissue quicker, and the ultrasound wave will not be able to penetrate as deeply into the medium as with a lower frequency.

Acoustic impedance

Another important material property in ultrasound imaging is the acoustic impedance. The acoustic impedance of a material describes how much resistance is encountered when a sound wave passes through medium and is determined by the density and stiffness of the medium. A medium with a high density is harder to accelerate than a medium with low density, due to there being a higher amount of mass in the same space. Also, a medium with a higher stiffness will be harder to accelerate than a medium with lower stiffness, since the particles will be harder to move. Acoustic impedance, z, can be calculated from the local particle pressure, p, and the local particle velocity, v, as in

$$z = \frac{p}{v}. \tag{2.2}$$

Reflection

To use acoustic sound as a measuring tool, a sound wave is transmitted and then the returning echoes are measured. The reflections are caused by a difference of acoustic impedance in interfacing mediums. How large the reflection will be is decided by the change of acoustic impedance. The sound wave will not only reflect, but also move forward and be partly transmitted into the new medium. The total intensity of the sound wave will not change, it will only split into one reflected sound wave and one transmitted sound wave. This behavior is a physical result in keeping the wave continuous and the medium undamaged. The sum of the reflected intensity and the transmitted intensity will be the same as the incoming original sound wave, with the assumption that no absorption occurs, see Figure 2.2.

The sum of the incoming and reflected pressure is the same as the total transmitted particle pressure, (2.3). The sum of the incoming and reflected velocities is the same as the total transmitted velocity of the sound wave, (2.4). Again, this is due to the wave having to be continuous with no material disruptions. By looking at Figure 2.2 and using (2.2), it is shown how the acoustic impedance of the different mediums decide how much of the wave will be reflected and how much will be transmitted.

$$p_i = p_t + p_r \tag{2.3}$$

$$v_i = v_t + v_r \tag{2.4}$$

From the above equations: (2.2), (2.3) and (2.4) a ratio known as the amplitude reflection coefficient, R_A can be calculated,

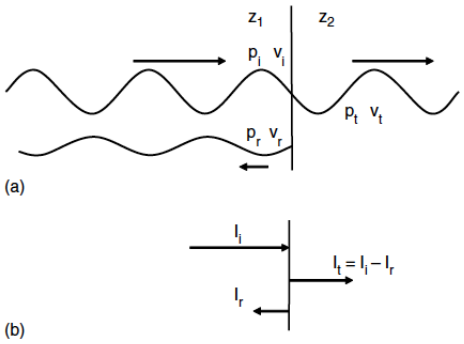

Figure 2.2: Illustration of how an incoming sound wave reflects at the interface to the second medium. (a) Shows the particle pressure and velocity and how the sound wave continues and reflects when passing from one medium with acoustic impedance z_1 to the second medium with acoustic impedance z_2. (b) Shows the relation of the intensity of the incoming wave and the resulting reflected and transmitted waves. From [11].

$$\frac{p_r}{p_i} = \frac{z_2 - z_1}{z_2 + z_1} = R_A. \tag{2.5}$$

Ultrasound images are built from reflections of ultrasound waves. The reason ultrasound images can be constructed is that the returning echoes have different amplitudes. It is this difference in amplitude that contains the information to create an ultrasound image.

Resolution

In all types of medical imaging the resolution of the image is important; medical images need to be adjusted for the specific cause of the examination. Whether a high resolution is needed to observe small objects and structures, or a change in contrast is needed of two structures are too similar, or if timing is important and the images need to be taken with a faster frame rate and lesser spatial resolution.

In ultrasound imaging the frequency of the ultrasound wave is an important factor of the resolution of the scanned image. The frequency specifies how deeply the ultrasound waves can penetrate and reflect back without too much attenuation occurring. The frequency and wavelength also gives the spatial resolution. The spatial resolution specifies the size of the smallest detectable object in the image. The typical frequency used in medical diagnostic ultrasound transducers is between 2-15 MHz. In Table 2.2 the corresponding wavelengths for typical diagnostic frequencies are shown.

Table 2.2: The wavelength of different frequencies in soft tissue, with an assumed speed of sound of 1540 m/s. Data from [11].

Frequency, f (MHz)	Wavelength, λ (mm)
2	0.77
5	0.31
10	0.15
15	0.1

In ultrasound imaging there are three important types of resolution: spatial, temporal and contrast. These three together determine the quality of the image. Spatial resolution is the ability to distinguish two points in an image. The choice of frequency determines how close two targets can be while the ultrasound still will be able to detect and and display these targets as two separate entities [13]. Shorter wavelengths improve spatial resolution, but have lower penetration depth.

Temporal resolution is important when scanning ultrasound images over time. It is the ability to accurately show changes in the scanned anatomy over time. Temporal resolution is the time from the beginning of one frame to the next frame. This depends on the depth of the scanned image, the further the ultrasound waves have to travel, the longer time it will take for the echos to return. The width, or number of scan lines, of the image also decides how long it takes for one image to be scanned. The more scan lines, the longer it takes to get one complete ultrasound image [13].

Ultrasound pulses vary in power, which is proportional to the squared amplitude. Contrast resolution is the ability to distinguish between different tissues which have different characteristics. These differences in characteristics can give different echo amplitudes, such that it can sometimes be difficult to distinguish adjacent structures [13]. The brightness, or the amplitude of the returning echo is determined by the reflection constant, R_A. Contrast resolution can be improved with different methods throughout the imaging process, using either compression, image memory and use of contrast agents.

B-mode imaging

The classical 2D image of ultrasound imaging is called a B-mode image. The B in B-mode image stands for brightness. A B-mode image is constructed by the reflected ultrasound transmitted by a transducer. The strength (amplitude) of the returning signal implies the brightness of the image. With increasing resolution in the images, smaller objects and movements can be

detected. [14]

To create an ultrasound pulse, a transducer with piezoelectric elements is used. Each one of these piezoelectric elements transmits an ultrasound pulse. At each new interface the ultrasound pulse is reflected back, and the transducer scans the returning echo. By knowing the time difference from transmitted and returning pulse the location of the interface can be calculated, and the strength of the signal gives the brightness at the spot. One single piezoelectric element would create a 1D line, and with several piezoelectric elements in a line these 1D images can be added together to create a 2D image. The adjacent piezoelectric elements are combined through superposition to create a wavefront. This wavefront can be changed by adding och changing the time delay between the transmitted pulse which are used to create the wavefront. See Figure 2.3 for an illustration of how this works.

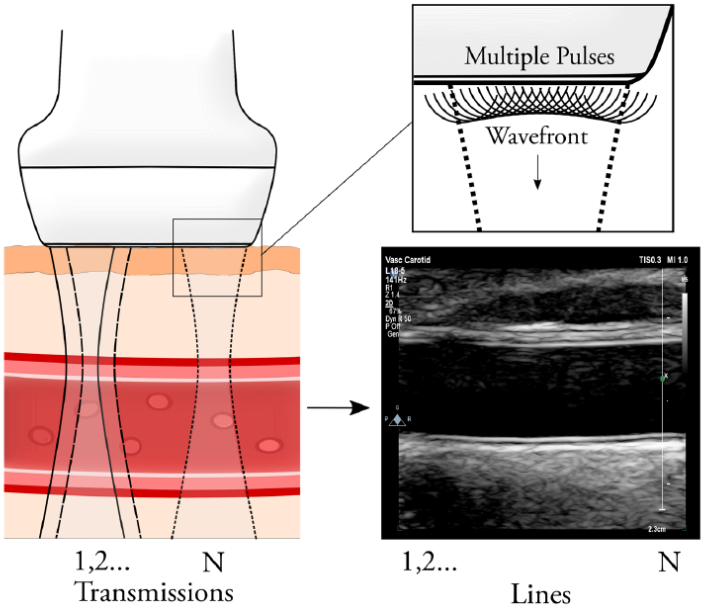

Figure 2.3: Illustration of how a B-mode ultrasound image is constructed. One line in a B-mode image corresponds to a single ultrasound transmission. To create a full image, multiple pulses are transmitted, resulting in a wavefront. The amplitude of the echoes of the wavefront are what determine the brightness of the pixel in the corresponding location of that echo. From [15].

There are several types of transducers for B-mode imaging, depending on what format is best for the specific application. See Figure 2.4. Here a linear transducer is the most common, the piezoelectric elements are all

in a straight line, and a rectangular image is produced, this can be used when there is need to view the superficial tissue as well as the deeper organs simultaneously.

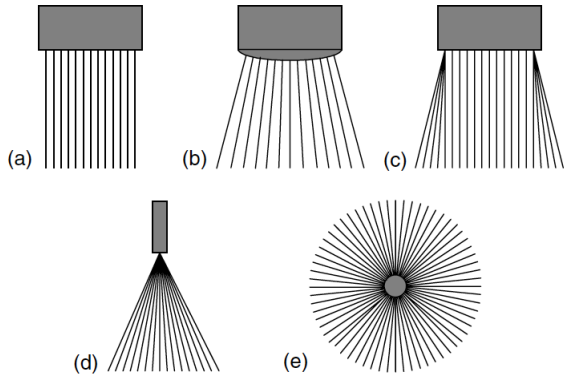

Figure 2.4: Illustrations of different types of 2D transducers used for B-mode imaging. (a) A linear transducer. (b) A curvilinear transducer. (c) A trapezoidal transducer. (d) A sector transducer. (e) A radial transducer. From [16].

3D and 4D ultrasound imaging

There are several different ways to create a 3D ultrasound image. The theory is mostly the same as in creating a 2D B-mode image, with an added dimension. There are 3D transducers, which contain a 2D matrix of piezoelectric elements and scan electronically over the scanning area to create a 3D image directly from data collection. Then there are methods which use a 2D transducer and the 3D volume is built up with scanned 2D images, see Figure 2.5.

For 4D ultrasound the next added dimension is time, it is a 3D motion image. These images are harder to create. They are created by using a mechanically steered array or a 2D transducer together with a specific time stamp. This can be done by either adding 3D images over time or instead by having 2D motion images added together sequentially over the third axis. These 2D motion images need to be timed correctly to put together a correct 4D image. This 4D construction method is time-consuming, and the fast process of e.g. a heart beat, is hard to capture. Therefor, one way to construct 4D images is by using an electrocardiogram (ECG). An electrocardiogram shows the electric signals of the cardiac cycle. By using the ECG of a person the 2D motion scanning can be triggered at a specific point on the cardiac cycle and set to sample for the wanted amount of

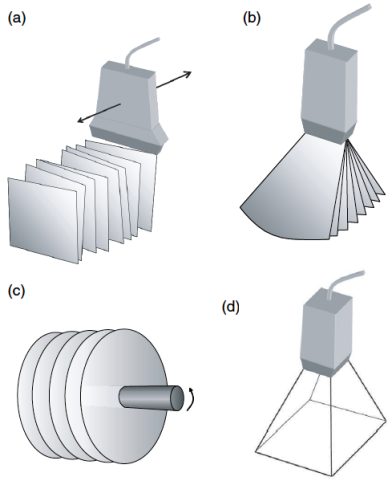

Figure 2.5: Illustrations of different types of 3D scanning methods used for 3D ultrasound imaging. (a) Freehand 3D scanning. The operator scans using free hand and the resulting 2D images from the scan build the 3D volume. (b) Mechanically steered real-time 3D. This scanner is mechanically scanning back and forth to scan 2D images to build the 3D volume. (c) Endoprobe 3D ultrasound. The endoprobe scans a sequence of 2D images parallel to one another to construct a 3D image. (d) Matrix array 3D ultrasound. The transducer has an electronically controlled beam which steers the beam to create a pyramid shaped 3D volume. From [17].

cardiac cycles. This way a correct 4D is created with the correct timing, even though the 2D motion images are not collected at the exact same time. More on ECG in section 2.2.1.

Visualizing 3D and 4D images on a 2D screen is difficult. There are no 3D displays, and looking at all the data at once will be hard to interpret. The easiest way to view 3D images is to look at the separate 2D images and construct each orthogonal image to create a cut-through of a 3D image. There is also a technique called shaded surface display, where the connecting surface of a chosen object is selected and then shaded. This is commonly used when viewing fetuses.

Doppler ultrasound

The Doppler effect can be applied to ultrasound systems to create Doppler ultrasound. This is used to detect the motion of tissue and blood in ultrasound images. The Doppler effect is most commonly described by using the example of an ambulance. The sirens of an ambulance send out sound waves

with a specific frequency. When an ambulance is driving towards you, the sound of the sirens has a higher frequency than if the ambulance would have been still. When the ambulance is driving away from you, the frequency of the sound will be perceived as lower than the still ambulance. The Doppler effect is described as being the change in frequency of the perceived sound wave compared to the original emitted sound wave.

Doppler ultrasound however works differently than the Doppler effect. Instead of comparing the change in frequency Doppler ultrasound measures the time difference for returning echoes. The transducer sends out multiple consecutive pulses. When the blood is flowing, as it should, the particles in the blood create a delay in the echo compared to their location in the previous image. This delay can through signal processing give us a velocity profile of the blood flow, through Doppler ultrasound, see Figure 2.6.

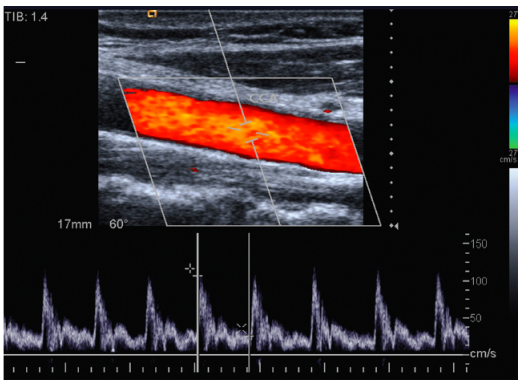

Figure 2.6: An image of what Doppler ultrasound looks like. This demonstrates both colour Doppler (the colour displayed in the image) and spectral Doppler (which can be seen in the bottom of the image). From [18].

2.2 The cardiovascular system

The cardiovascular system supplies the body with oxygen, nutrients and hormones and relieves the body of carbon dioxide and other metabolic waste. It is composed of the heart together with the blood and blood vessels. The hearts function is to pump blood to all the cells in the body using a vast network of blood vessels. The heart has four different valves, the right and left atrium as well as the right and left ventricles, see Figure 2.7. Blood flows from the veins into the atrium and then continues to the ventricle then leaves the heart through either the aorta or the pulmonary artery. From the body, blood returns to the heart through the vena cava or

the pulmonary artery. A vein is a blood vessel leading blood back towards the body, and an artery is a blood vessel which leads blood away from the heart. The inside of the blood vessel where the blood flows is called lumen.

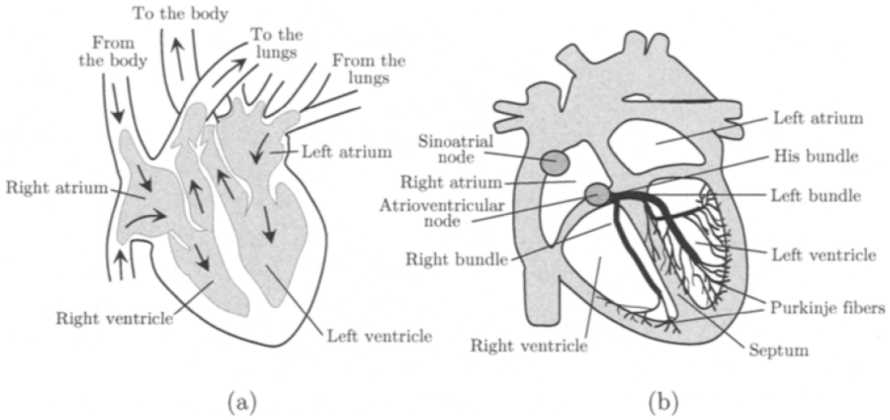

Figure 2.7: Illustration of the heart. (a) Illustrates how the blood flows through the heart. (b) Shows the electrical grid of the heart muscles. From [19]

2.2.1 ECG and the cardiac cycle

The cardiac cycle (one heartbeat) consists of two parts, systole and diastole. Systole is when the heart is compressing and pumping out blood and diastole is when the heart is relaxed and filling with blood. The heart muscle contractions start with an electrical impulse which propagates through a network of electrical signals for the most effective pumping motion. An image of the heart and its electrical grid can be seen in Figure 2.7. The heart contractions start at the sinoatrical (SA) node, which is the pacemaker of the heart and controls our pulse and blood flow. The electrical impulse which originate at the SA node spread throughout the heart muscles for a coordinated pumping movement. From the SA node the pulse propagates through the electrical grid so that both atria contract simultaneously and press the blood into the ventricles. How this electrical pulse is spread can be viewed in an electrocardiogram (ECG). In a healthy heart the ECG rhythm is comprised of five distinct curves, an example of which can be seen in Figure 2.8.

2.2.2 Blood vessel anatomy

The arteries have to withstand more pressure than the veins, and are therefore thicker. The arterial walls are made up of three different layers, the

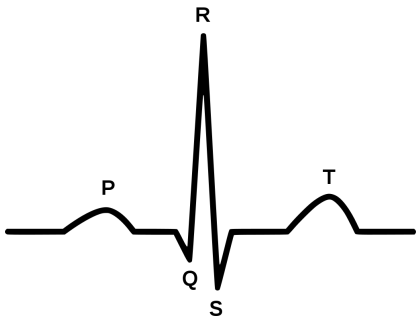

Figure 2.8: A typical ECG of one cardiac cycle. The different curves have different names, to be able to describe different features or anomalies which might be found within an ECG. From [20].

tunica externa/adventitia, tunica media and tunica intima, see Figure 2.9. The tunica adventitia is the outermost layer and consist mostly of collagen fibers to reinforce and protect the blood vessels. These fibers are also connected to surrounding tissue to hold the vessel in the correct place. The tunica media is the middle layer and the thickest layer. Here there are a lot of smooth muscle cells as to regulate the diameter of the lumen, depending on situation. The tunica intima is the innermost layer and it is also the thinnest layer. This layer contains the endothelium, which varies in thickness. The thinnest this can be is one layer of cells thick in the arterioles. The tunica intima is much thicker in the larger arteries and in the aorta. The purpose of the endothelium surface is to provide structure and low friction for the blood flowing in the vessels.

The commmon carotid artery (CCA) is the main artery which supplies the neck and head with blood. There is one on each side of the neck, the left CCA and the right CCA. In this thesis it is the CCA which has been used for analysis.

2.2.3 Arterial wall movement

When blood flows through the body, the rate of the blood flow and the blood pressure is not constant, but changes due to the heart rhythm. Other physical factors can also affect how the blood flows. This can, in turn influence the blood vessel wall movement. There are known physical factors which affect the diameter in the arteries of the lumen, such as stress, which expands the diameter to allow for larger blood flow to transport more oxygen in the case of a stressful situation. The arterial wall moves in two directions, the radial direction and in the longitudinal direction, see Figure 2.10. Measurements on these movements have been done in both directions, however until the beginning of the century the longitudinal movement has

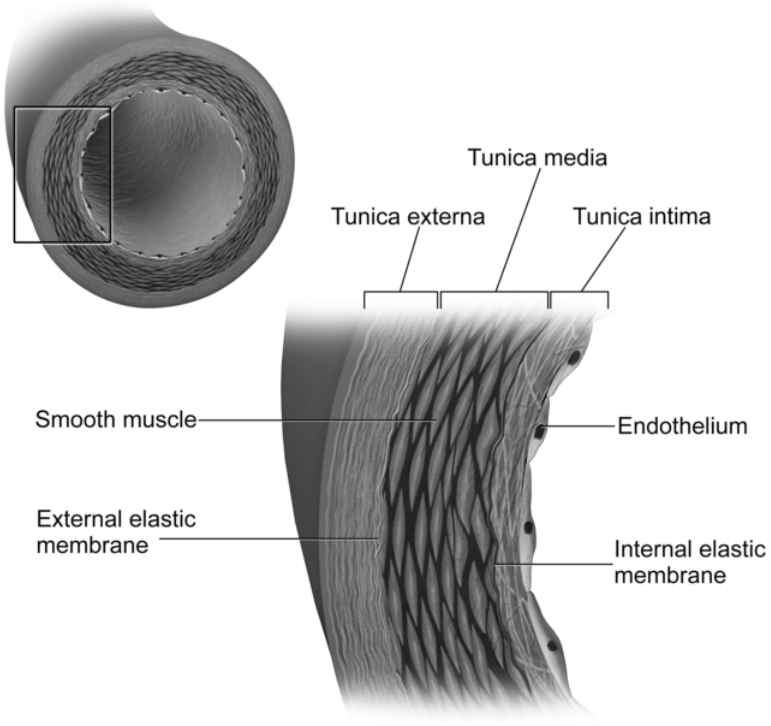

Figure 2.9: Image of the cross section of an artery, illustrating the three different layers and their composition. From [22].

been thought to be negligible [2][21].

Radial motion

There is extensive research on how arterial wall movement is affected in the radial direction due to physical factors such as age and cardiovascular diseases. Arteries expand and contract radially, in a pattern correlated to the cardiac cycle [15]. Measurements with non-invasive ultrasound can be used to view this motion and investigate the mechanical functions of the arterial wall [23]. Both instantaneous diameter change and the elasticity of the vessel-wall are markers of increased morbidity [21]. With the help of these markers we are able to detect the increased risk or the presence of cardiovascular diseases. Increased stiffness in arteries can reflect the possibility of atherosclerosis, Marfan syndrome, hypertension, diabetes, coronary artery disease, myochardial ischemia and infarction as well as chronic heart failure [21]. The movement of the radial wall is typically in the mm span [24].

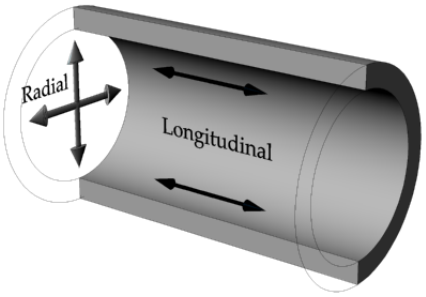

Figure 2.10: An illustration of how the two different movements are defined in arteries. From [15].

Longitudinal motion

Longitudinal movement in the arterial walls was discovered much later than the radial wall movement. At the Biomedical Engineering Department at Lund University, they have studied this movement, together with the Department of Translational Medicine at Lund University, with the help of high resolution ultrasound [2]. The intima media complex of the arterial wall has a much larger longitudinal motion, than movement of the tunica externa [2]. This is shown by Persson et al. (2003), and an example of this motion can be seen in Figure 2.11.

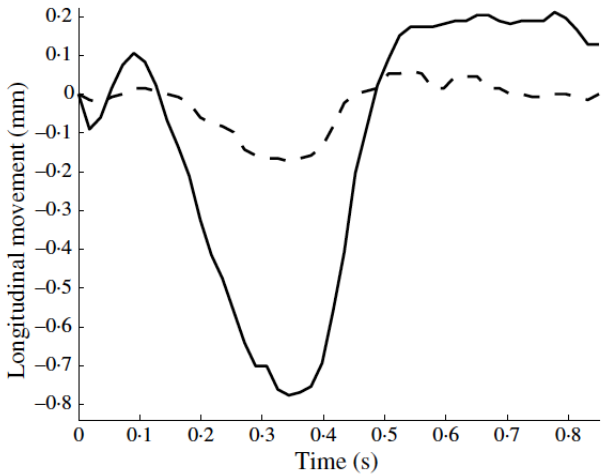

Figure 2.11: An example of the longitudinal movement of a healthy female. The dashed line shows the motion of the tunica externa and the solid line shows the motion from the intima-media complex. [2].

Since the significant movement occurs in the intima-media complex high resolution ultrasound is necessary to detect the motion of the different layers of the arterial wall. Figure 2.12 shows the intima-media complex of the arterial wall in ultrasound images of the common carotid artery.

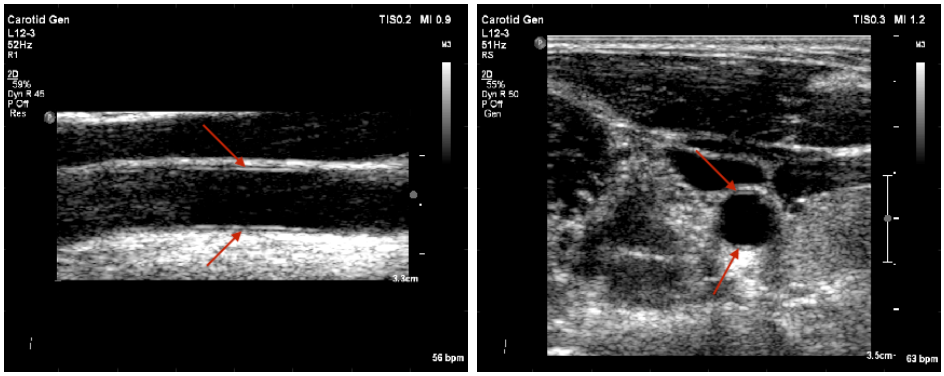

(a) **(b)**

Figure 2.12: Ultrasound images of the common carotid artery viewed in two different directions, longitudinal 2.12a and radial 2.12b. The red arrows indicate the position of the intima-media complex of the arterial wall.

Because the radial movement of arterial walls can give pathophysiological information, it would stand to reason that the longitudinal motion might also be able to give some information about the pathophysiological process of vascular diseases. There is currently ongoing research to try and establish markers of early detection of cardiovascular diseases correlating the longitudinal motion of the arterial wall. In studies done with porcines, Ahlgren et al. (2012) has shown that the longitudinal motion increases under the stimulant of catecholamines (neurotransmitters such as dopamine, adrenalin and noradrenalin). Later, Ahlgren et al. (2015) found that the increased longitudinal movement takes place independently from the wall shear stress from the blood flow. Wall shear stress is the force on the vessel-wall from the blood flow and pulse waves. These are both important findings for understanding the how the longitudinal motion correlates to cardiovascular diseases. Cinthio et al. (2018) discovered that the longitudinal motion is multi-phasic, and that the specific movement pattern varies depending on the individual, but that it increases with age. Multi-phasic movement means that the movement occurs in different phases, with different directions. The longitudinal movement where the arterial wall moves with the blood flow is called antegrade movement. The longitudinal movement where the arterial wall moves in the opposite direction of the blood

flow is called retrograde movement. An image of multi-phasic longitudinal movement plotted together with the radial movement and the simultaneously measured ECG can be seen in Figure 2.13. The typical size of the longitudinal movement is around one millimeter, but this also varies from individual to individual.

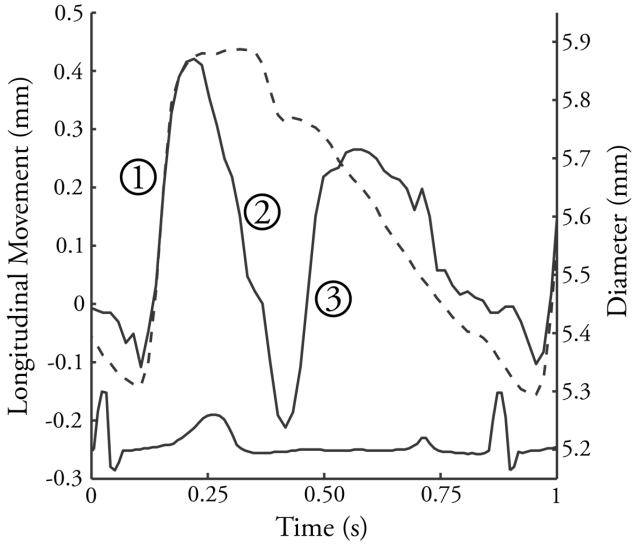

Figure 2.13: An example of the longitudinal movement plotted together with the radial movement and the measured ECG. The dashed line shows the radial movement and the solid line shows the longitudinal movement. The longitudinal movement is composed of an antegrade movement (1), a retrograde movement (2) and another antegrade movement (3). [15]

In Figure 2.13, the multi-phasic pattern is clearly visible, here it is triphasic. It is initiated with an antegrade movement, which then is followed by a retrograde movement which in turn is followed by an antegrade movement, before the arterial wall returns to its original position.

2.2.4 Blood flow

The blood flow in arteries follows different flow patterns [23][25]. These patterns can be analyzed with the help of Doppler ultrasound or MRI (magnetic resonance imaging). The dynamics of blood flow is called hemodynamics. How the blood flows in the arteries can change depending on vascular diseases [8]. The friction of vessel-walls affects the velocity profiles such that the flow is slower at the walls, so that the velocity profile becomes parabolic. Laminar blood flow, when the liquid flow follows a straight path, is usually

a marker for healthy arteries. In the case of atherosclerosis there is a flow reversal, due to the narrowing of the artery [25]. Before 3D imaging was available only 2D blood flow profiles were available. With 3D motion imaging techniques, such as MRI, it can be seen that the blood flows in a helical profile at the carotid bifurcation (where the carotid artery splits)[26]. This means that the blood flows in a spiral shape. Using a 4D MRI imaging technique, Harloff et al. (2009) compared the blood flow of healthy volunteers to the blood flow of patients with internal carotid stenosis (atherosclerosis). It was found that the healthy volunteers had a helical blood flow profile at the carotid bifurcation and the patients with stenosis had a more turbulent and varied flow.

2.2.5 Cardiovascular diseases

Cardiovascular diseases (CVDs) are the cause of 31 % of all global deaths and are the leading cause of death in the world. Out of the different cardiovascular diseases stroke and heart attack are the most common, leading to 85% of cardiovascular related deaths [1]. Most of these deaths occur in poor countries, where the cost for health care is too high, and there are no easy cheap methods to find and prevent cardiovascular diseases [1]. Even though there has been significant research and progress to understand the pathophysiological process underlying these diseases, there is much knowledge to gain before we can have a complete understanding of the different cardiovascular diseases.

Cardiovascular diseases are split into five categories with three of them being peripheral arterial disease, cerebrovascular disease and coronary heart disease. Peripheral arterial disease is when the blood vessels supplying the arms and legs are injured or damaged. Cerebrovascular disease is when blood vessels supplying the brain are injured or damaged. Coronary heart disease is when the blood vessels supplying the heart muscle are injured or damaged. In all of these it is essential to have vast knowledge on the pathophysiological process of these diseases. Most importantly is being able to detect these diseases at an early stage. Early detection increases the chance of surviving and having a higher quality of life. As previously written, the elasticity of central arteries can show a connection to cardiovascular diseases, such as atherosclerosis, coronary artery disease, myochardial ischemia, myochardial infarction and chronic heart failure. Atherosclerosis is the build-up of plaque in the arteries, which leads to a thicker and stiffer arterial wall [27]. Other diseases also affect the mechanical functions of the arteries. These are Marfan syndrome, hypertension and diabetes [28]. Hypertension is not a disease in itself, it is actually high blood pressure which can lead to severe health problems and increases the risk for cardiovascular

diseases [29].

Considering the above, more research on the how the longitudinal movement in arteries is affected by cardiovascular diseases could give important information that could effectively reduce morbidity. It could also help with the prevention of cardiovascular diseases, decrease the amount of deaths related to cardiovascular diseases and reduce the amount of resources used in relation to cardiovascular disease. Currently no one has been able to measure the movement of the arterial walls in 3D or 4D, and it is of great interest to develop such methods to gain as much information as possible about the cardiovascular system and the movement of the arterial wall.

Chapter 3
Method

In this chapter the methods used for this thesis will be presented. In this thesis there was not a set path for achieving results, there was some trial and error where the plans and methods had to change. This description of the method will contain a description of the whole process, from start to finish, including original thoughts and how the process and method developed until final results.

Firstly, a description on how the imaging samples for movement tracking were acquired is presented. Then continuing on with a description of the functions of the different parts of the GUI. The ultrasound machines used for this thesis were Vevo 3100 High-Resolution Imaging System (Visualsonics Inc, Toronto, Canada) and Philips EPIQ 7G (Philips Medical Systems, ATL Ultrasound, Bothell, WA, USA) with a 3-12 MHz linear array transducer. All post processing was done on a computer using MATLAB (The Mathworks Inc., Natick, MA).

3.1 Experimental set-up for collecting data

The purpose of this thesis was to analyze the 3D motion of the carotid artery. Thus 3D ultrasound films had to be sampled.

This was the first time the department tried to capture 4D ultrasound images of the carotid artery. This of course led to unforeseeable issues. The first problem was to figure out how to capture the desired data. A normal ultrasound transmitter captures a 2D image, which can be viewed either as a single still image, or as 2D images over time (2D film).

The only available ultrasound transducers suitable for vascular imaging, were for 2D imaging. Since no matrix array 3D ultrasound transducers were available, 2D motion images would have to be scanned separately and afterwards be built into a 4D volume. These images have to be scanned with a certain time-stamp. With the help of an electronically steered step-motor, controlled steps could be taken with the transducer, and 2D motion

samples over a specific time-stamp were acquired. This process is repeated until the correct amount of samples were acquired to build the desired size of the 4D image.

The motion tracking of the data samples would be on arterial walls, and a suitable time-stamp is to use the cardiac cycle. The sampling would start at the beginning of the cardiac cycle and last for two cycles. Then the acquired images would supposedly be taken with the same-time stamp. For this to work the machine needed to connect to an ECG reader, and would have to trigger on the beginning of the cardiac cycle in the ECG and last for the desired number of cardiac cycles and then stop sampling.

The original plan was to use the ultrasound machine Vevo 3100, which has a computerized step-motor to control how large steps the transducer was translated between acquisitions, and the length of the 3D images. This had been previously used to take good quality 3D ultrasound images. However the goal was to collect 4D images (3D images over time), and there was no setting for this. This machine had an ECG reader, however when we tried to use this ECG reader on a test subject the machine would only trigger on ECG with a pulse higher then 180. (The normal resting pulse for an adult human is between 60-80 beats per minute). This machines ECG would only trigger on small mammals with a much higher pulse.

Thus the ultrasound machine Philips EPIQ 7G which had an ECG for human heart rhythm was used. However, since this machine did not have a motorized step sampler, a combination of the two machines were used for collecting the data. The machine with the built in motorized step sampler, Vevo 3100, would then be used for controlling the 3D steps. The Philips EPIQ 7G transducer was connected to the Vevo 3100 step-motor, and the steps and step-size controlled from Vevo 3100. Philips EPIQ 7G would then be used for ultrasound imaging collecting and ECG triggering, and one ultrasound 2D motion image was collected at each step taken with Vevo 3100.

Three healthy volunteers were used as test subjects in this pilot study and the data was sampled the same way for all three. They were all in a right lateral recumbent position (laying on their side with the right side facing down). The common carotid artery was found manually with the ultrasound transducer and then the transducer was set in the computerized step motor. Before sampling the data the step size and length of the 3D motion image was adjusted, so that it was certain that the common carotid artery would be seen throughout the data sampling.

Two different sets of images were collected from each test subject. One with a transverse cross-section view of the common carotid artery, and one with a longitudinal view of the common carotid artery. For the longitudinal image, the transducer was moved from the back of the neck going to the

front, and with the right side of the image being in the direction of the head of the test subject. For the transverse image, the transducer sampled the images from the lower part of the neck going up towards the head, and with the left side of the image being the towards the front of the body.

3.2 MATLAB coding for viewing the images

Prior to collecting the real 4D images, some sample images were supplied by the thesis supervisor. This first set of images were taken by the originally intended ultrasound machine Vevo 3100, and these images were sampled in an IQ format, where IQ stands for in-phase quadrature. A GUI was created to view these 3D images in the purpose of practicing before the 4D images were sampled, to be sure that the program created would be compatible with those image formats.

However, when the data sampling did not work with the originally intended ultrasound machine and the machine doing the ultrasound sampling changed, the file format for the collecting ultrasound images also changed. The files were now in a DICOM format and a new GUI was created. These DICOM images were scaled down from their original size to minimize the size of the 4D image used later on in the tracking algorithm. The DICOM format is commonly used for storing medical images and related data.

The sampled 4D images were taken with different sample rates for each volunteer, but was the same throughout all scans for each individual 4D image. The heart rate and ECG varied, and each 2D motion image ended up having varying amounts of scanned images, due to the ECG being of different lengths. The extra scanned images were simply cut off at the end.

Viewing the images in 3D proved to be difficult, there are not many functions to view whole 3D images in MATLAB. However, MATLAB has built in functions for viewing 3D objects and surfaces. After trying and evaluating different functions, the decision was made to segment and view the segmented arterial wall in 3D using a surface plot. Instead of viewing the whole 3D motion image in its entirety, a step function for viewing the different depths and frames in 2D was put into the GUI.

3.3 Segmentation of the arterial wall

To be able to view the arterial wall in 3D, the wall was segmented into a non-symmetric cylinder shape. This was done manually in the GUI. Only the first frame (time step) was segmented, to use as an original shape of the arterial wall. It is easier to segment the arterial wall when viewing the artery radially, so 2D slices of the vessel viewed in a transverse direction

were segmented in first time frame. For each one of these images a manual segmentation was done around the arterial wall, starting at the bottom of the intima-media complex. The manually selected coordinates were then equally spaced around the segmented shape, an algorithm was created for this purpose. This algorithm also enables one to choose the amount of coordinates spaced around the segmented shape. Even after this the whole segmented shape was quite jumpy. To try and see if the results would be better if the arterial wall was more smooth, an averaging method was done on all the coordinates. This was done by comparing the current coordinate with the other coordinates longitudinally and taking an average of the closest coordinates. To view the segmented shape a surface plot was used in MATLAB.

3.4 MATLAB coding for movement tracking

The algorithm for movement tracking was further developed from supervisor Tobias Erlöv's motion tracking algorithm, phase shift tracking, [9], by adding a third dimension.

This motion tracking method compares phase shift of the pixels in adjacent images to see the how much that pixel has moved. This is done by using the Hilbert-transform (HT) on the 3D matrices. The HT returns information about the local phase of the signal, i.e. if the signal is sinusoidal the local phase of adjacent samples would increase linearly from 0 to 359 degrees, then start over at 0 and so on. The nice thing about ultrasound images is that the amplitude pattern (the speckle) is usually rather well approximated as sinusoidal. Hence, if the local phase of adjacent samples were to be plotted (and removing the phase shifts from 359-0) a fairly straight line would appear. Thus, the gradient of the local phases of the amplitude data (ultrasound image) can be estimated by the equation of a straight line. By knowing the gradient of the local phase, comparing the linear equations and knowing the difference in phase for each pixel in two adjacent frames the motion for each pixel between two frames can be calculated.

3.5 Final GUI and viewing results

Viewing the results in a 3D format was difficult. The movement tracking algorithm generated a 4D matrix with the motion for each pixel. To apply and view the results of the motion tracking algorithm, the resulting motion was applied to the segmented arterial wall shape. Applying the motion to the arterial wall segment was done one time-frame at a time. The corresponding motion of the coordinates of the original arterial wall segment,

was applied to each coordinate to create the second arterial wall segment. This process continued for all time-frames, with a "new" generated arterial shape for each step.

Using the surface plot function in MATLAB together with either a vector function for displaying movement, quiver3, or together with a colored surface for showing the movement in color, the segmented 3D surface could be viewed in motion. The segmented shapes were plotted sequentially in the same figure, so as to give the illusion of a moving segmented arterial wall. No specific results could be drawn from this way of viewing the 3D motion images, and so two other ways to view and compare the results were done. The first method to check the movement tracking was to apply the results from the movement tracking of each semi-circle to each 2D motion image and see if the coordinates moved together with the arterial wall. The second was to chose some coordinates in the image and plot the motion for those coordinates.

To compare the results of the 3D motion tracking algorithm, a couple of 2D motion images were selected as reference images. These 2D motion images were then analyzed with the help of a program called ARTIC developed by Nilsson et al. (2014). ARTIC evaluates the motion of the ultrasound images in 2D by using the same principle of phase shift tracking [30], but enhanced with knowing the location and gradient of the vessel wall. These reference plots were then compared to the results from 3D motion tracking, comparing the motion of the radial (y-axis) and longitudinal (z-axis) directions.

Chapter 4
Results

In this chapter the results from this thesis will be presented. Only a handful of images and plots for each test subject will be shown. These are chosen to give the reader an understanding of the final results and how they were produced. The results will be discussed in the next chapter.

4.1 Segmentation

In section 3.3 a description of the manual segmentation was given. An example image of a segmented section can be seen in Figure 4.1. The different axes are labeled so as to give the reader an understanding how the segmented shapes are aligned.

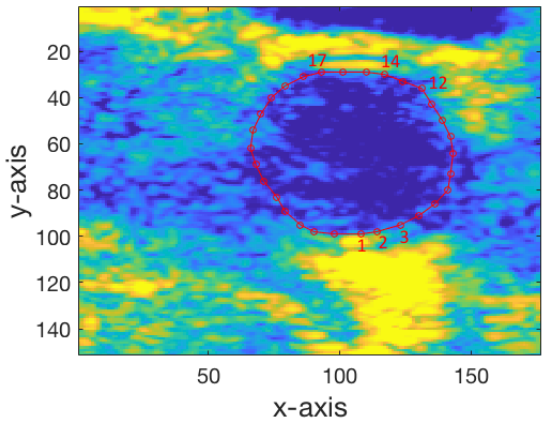

Figure 4.1: A segmented slice of volunteer 1. The red circles are coordinates for the segmentation around the arterial wall. The top and the bottom of the segmentation show the intima-media complex. The dark blue within the segmented shape shows the lumen. The size of one pixel is 0.078x0.078 mm^2.

A few example coordinates, as reference on which coordinates were chosen for movement tracking, are shown. The coordinates are aligned in the same way for all volunteers, and each segmented slice has the same amount of coordinates, in this thesis 31 coordinates are used for each segmented slice. From the segmented slices a complete segmentation of the first time-step of each volunteer was created. These segmented shapes of the three volunteers can be seen in Figures 4.2, 4.3 and 4.4.

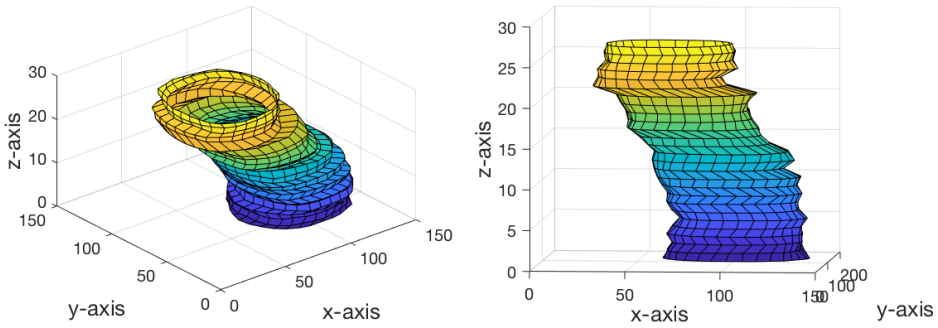

(a) **(b)** .

Figure 4.2: The complete segmented arterial wall for volunteer 1. The coloring is to view the 3D silhouette easier. Step size is 300 μm, number of steps taken is 27 (z-axis). The pixel height (y-axis) and pixel width (x-axis) are of the same size: 0.078 mm.

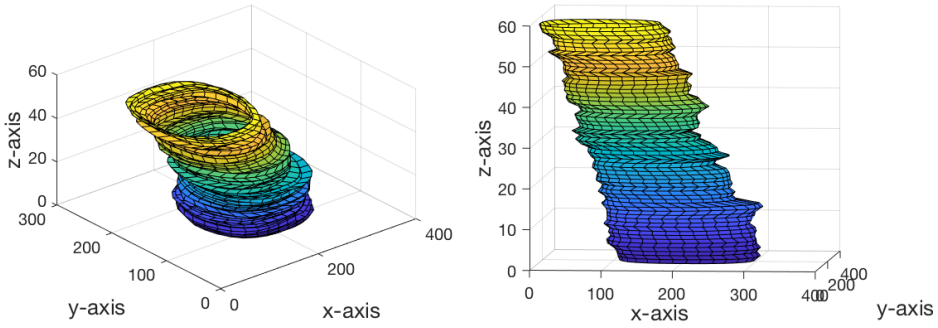

(a) **(b)** .

Figure 4.3: The complete segmented arterial wall for volunteer 2. The coloring is to view the 3D silhouette easier. Step size is 250 μm, number of steps taken is 59. The pixel height (y-axis) and pixel width (x-axis) are of the same size: 0.038 mm.

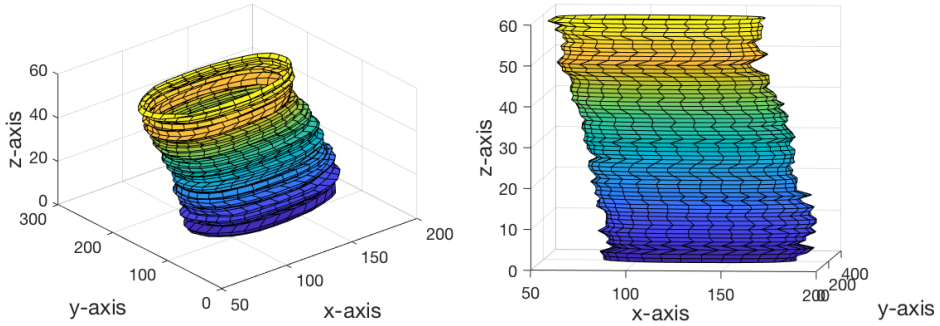

(a) **(b)** .

Figure 4.4: The complete segmented arterial wall for volunteer 3. The coloring is to view the 3D silhouette easier. Step size is 250 μm, number of steps taken is 60. The pixel height (y-axis) and pixel width (x-axis) are of the same size: 0.068 mm.

The step size of the first volunteer was 300 μm, and the step size of the second and third volunteers was 250 μm. In all of the segments, the positive z axis is in the direction of the head, and the positive direction of the y axis is aligned towards the left side of the body.

4.2 Tracking validation

The results of the tracking algorithm were firstly shown with a tracking validation code, 3.5. This was created mainly to see if the tracking algorithm worked. Here the coordinates of a segment slice were plotted on top of the corresponding 2D slice from the 4D image. An example of these can be seen in Figure 4.5 .

In the images from Figure 4.5 it is seen how the coordinates move together with the arterial wall. In Figure 4.5 the size of the jumps between the viewed frames are 15 steps. These tracking validation images are taken from volunteer 1. The total number of frames are 66 for volunteer 1.

4.3 Movement plots

The movement plots were created by choosing specific coordinates from the moving segments and plotting how much these coordinates moved in mm over time. For both the radial and longitudinal movement plots the first and last couple of depth frames were removed when plotting the average movement over time.

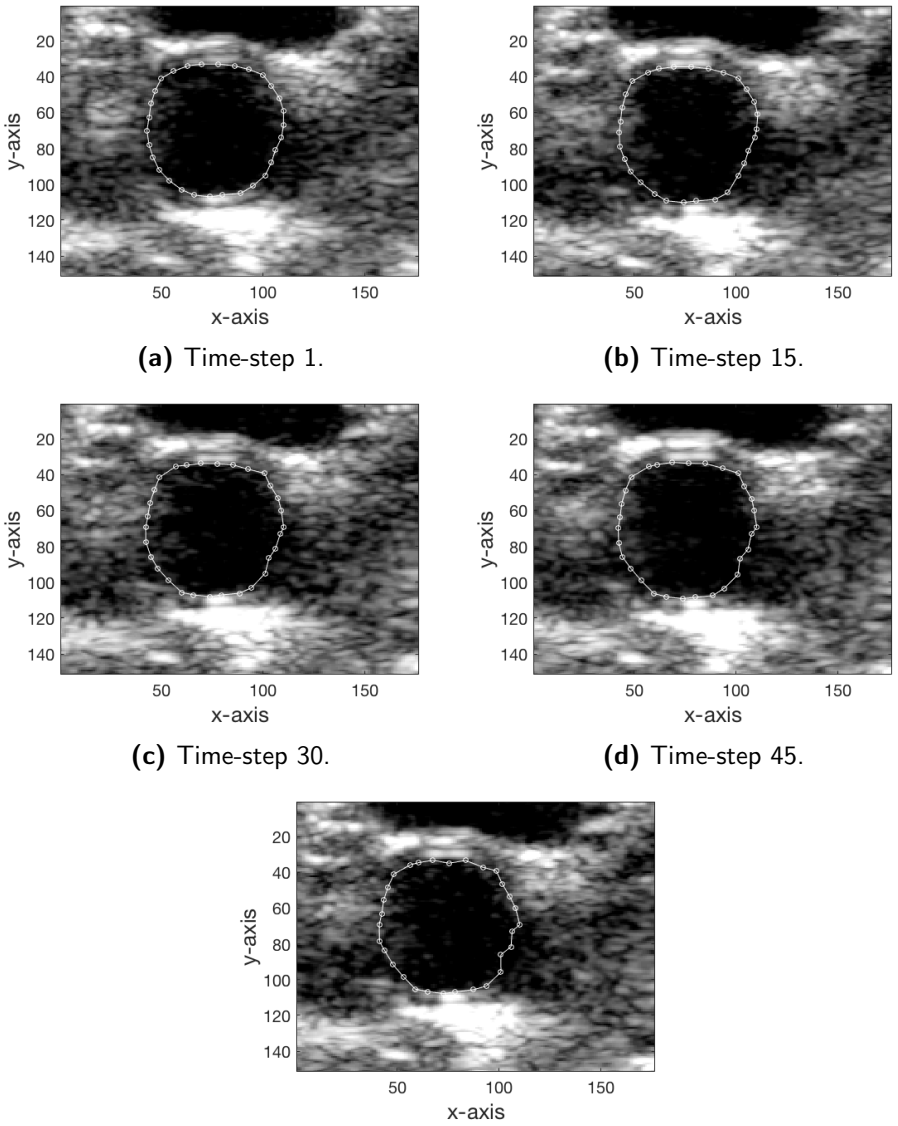

(a) Time-step 1.

(b) Time-step 15.

(c) Time-step 30.

(d) Time-step 45.

(e) Time-step 60.

Figure 4.5: Slices of the segmentation on top of the corresponding slices from the 4D image from four different chosen time-frames. The size of one pixel is 0.078x0.078 mm^2.

4.3.1 Radial movement

The radial plots each show the measured radial movement of the segmented shapes. This is done by comparing the top coordinates at the intima-media

complex at the top of the arterial wall in the segmented slice, and the bottom coordinates at the intima-media complex at the bottom of the arterial wall in the segmented slice, see Figure 4.1. For all radial movement plots the top coordinates used were 1 through 3 and 14 through 17. The radial movement plots for each volunteer can be seen in Figures 4.6a, 4.6b and 4.6c.

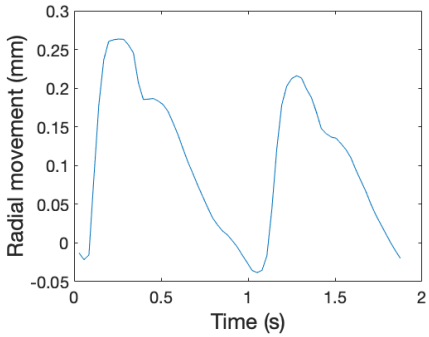

(a) Volunteer 1.

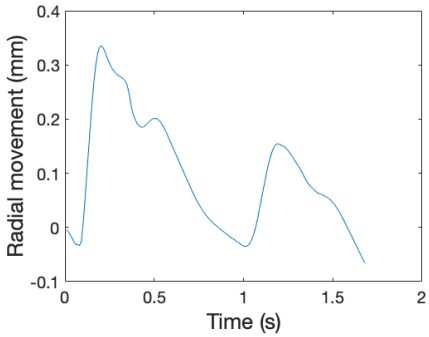

(b) Volunteer 2.

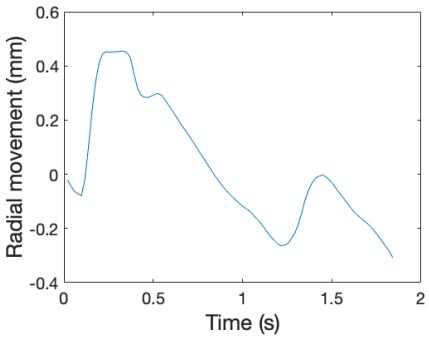

(c) Volunteer 3.

Figure 4.6: The radial movement measured in mm over time (s), over two cardiac cycles of all three volunteers. Measured with the 3D motion tracking algorithm. The motion is calculated by comparing the coordinates 1-3 and 14-17. The depth frames used for volunteer 1 4.6a are 7 to 20 and for volunteer 2, 4.6b, and volunteer 3, 4.6c, are 10 to 50.

4.3.2 Longitudinal movement

The longitudinal movement plots each show the measured longitudinal movement of the segmented shapes. This is done by choosing a couple of coordinates of the segmented shape. All three ultrasound 4D images vary, each with different dark areas, so the chosen coordinates for the three volunteers are chosen with some variety. One example from each volunteer will

be shown, these coordinates are chosen because they displayed the most similarities to the reference movement. All of the chosen coordinates are in the visible intima-media complex region, or very close to it. This motion tracking occurs between different tissue structures of the intima-media complex, which is the reason for high resolution needed when performing motion tracking, whereas for the radial tracking the entirety of the arterial wall is used. The results from the three volunteers can be seen in Figure 4.7.

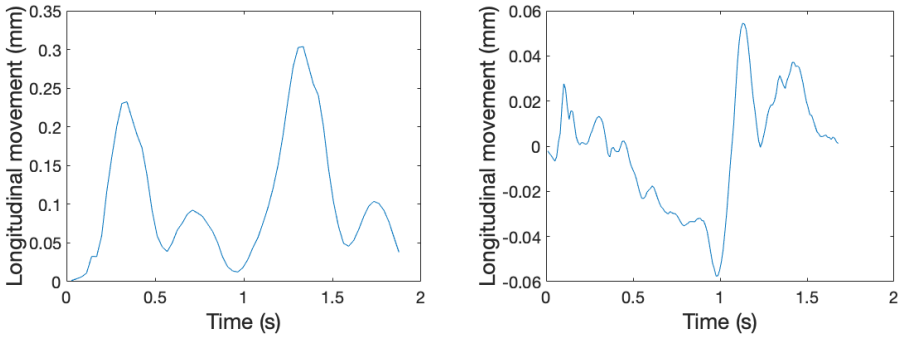

(a) Volunteer 1. Coordinates used for movement tracking are 1 to 3.

(b) Volunteer 2. Coordinates used for movement tracking are 14 to 17.

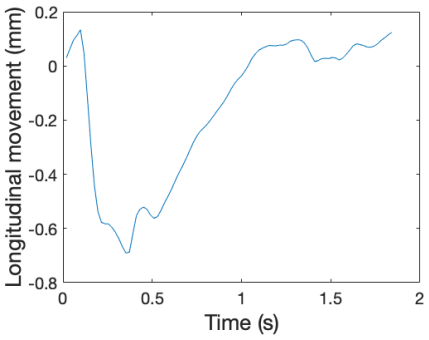

(c) Volunteer 3. Coordinates used for movement tracking are 14 to 17.

Figure 4.7: The longitudinal movement measured in mm over time (s), over two cardiac cycles of all three volunteers. Measured with the 3D motion tracking algorithm. The motion is calculated using different coordinates for each volunteer. The depth frames used for volunteer 1 4.7a are 7 to 20 and for volunteer 2, 4.7b, and volunteer 3, 4.7c, are 10 to 50.

4.4 The GUI

The results from Sections 4.1 and 4.2 are images that were produced by the GUI. The GUI was constructed and had various functions, including displaying different slices of the 4D image, movement tracking on the 4D image, manually segmenting the image, constructing a segmented arterial shape of the segmented slices and viewing the applied movement tracking on the segmented arterial shape. For an overview of the GUI see Figure 4.8.

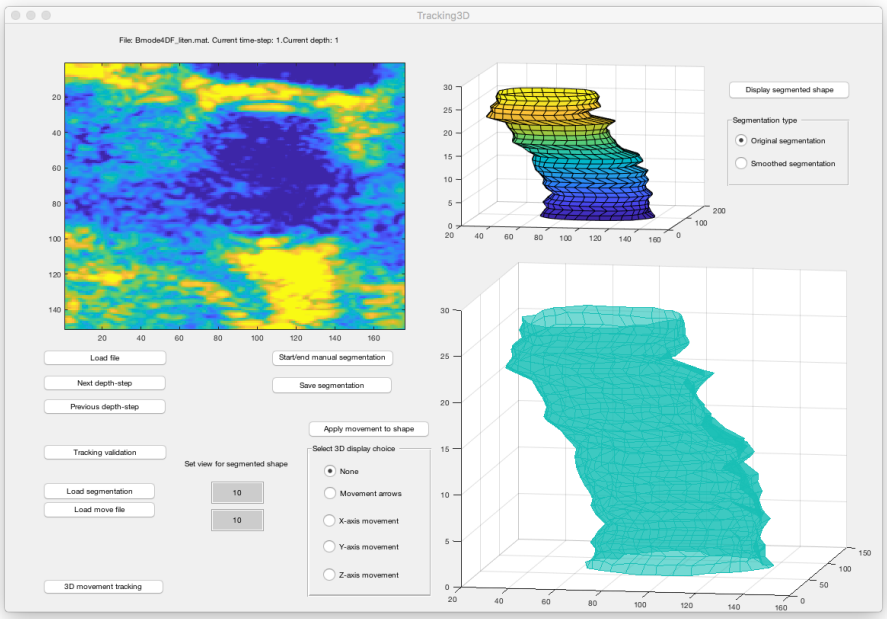

Figure 4.8: An overview of the GUI created for this thesis. The top left corner displays a chosen slice of the 4D image. The top right corner displays the segmented artery. The bottom right corner displays the movement sequence in 3D.

4.5 Reference plots

Here are the results from the selected images chosen as reference plots, created by using ARTIC [30]. ARTIC uses one 2D motion ultrasound image viewed longitudinally, to track both radial and longitudinal movement. ARTIC finds the gradient of the slope of the intima-media complex, and uses this in the tracking. Otherwise the tracking will only be performed in the image x and y axes, and not in the actual direction of the movement.

The resulting reference plots for the radial movement for the three different volunteers can be seen in Figures 4.9a, 4.9b and 4.9c, respectively.

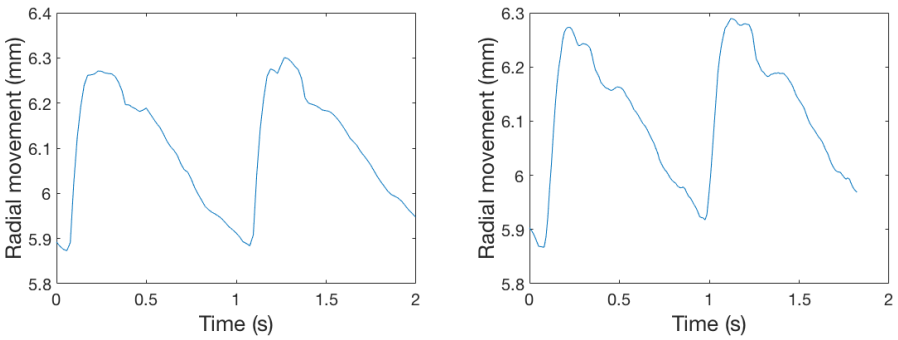

(a) Volunteer 1.

(b) Volunteer 2.

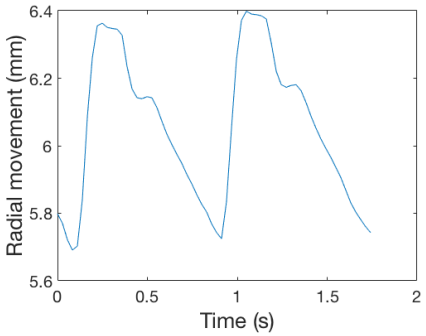

(c) Volunteer 3.

Figure 4.9: The reference plots of the diameter change (radial movement) measured in mm over time (s), over two cardiac cycles of all three volunteers. Measured with ARTIC [30].

The resulting reference plots for the longitudinal movement for the three different volunteers can be seen in Figures 4.10a, 4.10b and 4.10c, respectively.

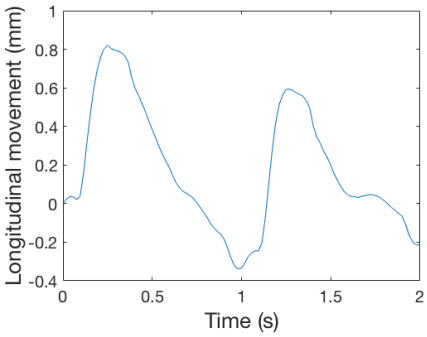

(a) Volunteer 1.

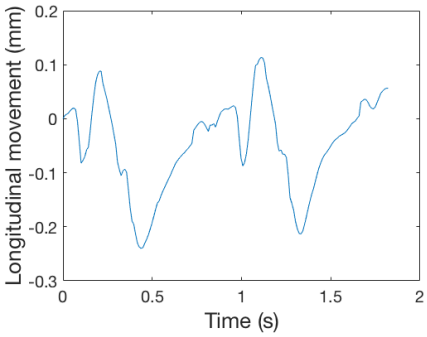

(b) Volunteer 2.

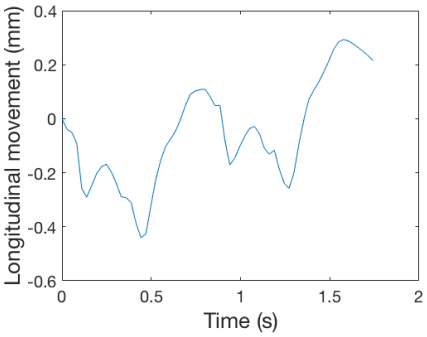

(c) Volunteer 3.

Figure 4.10: The reference plots of the longitudinal movement measured in mm over time (s), over two cardiac cycles of all three volunteers. Measured with ARTIC [30].

Chapter 5
Discussion

In this section the results will be discussed. Future work and conclusion for this thesis will be seen in the next chapter.

5.1 Comparing results

Looking at the results it can be seen that this implementation of movement tracking in 3D is not without fault. The tracking validation shows, Figure 4.5, that the coordinates do follow mostly in the x and y directions, except for in the darker areas.

When comparing the reference plots taken by ARTIC [30] to the resulting movement plots of this thesis 3D tracking algorithm, it is seen that they do differ from on another.

Volunteer 1

Looking at volunteer 1, the radial movement measured from the 3D tracking algorithm, Figure 4.6a, and the radial movement from ARTIC, Figure 4.9a, you can see that they do follow the same movement pattern. The second peak is a little lower and the movement tracking has lost a little in the second cardiac cycle, but you can still clearly see similarities. The magnitude of the movement is not the same. The reference plot shows that the change in radial movement is around 0.4 mm large, and the radial movement from the 3D tracking algorithm is around 0.3 mm large. This is a little less than the correct size, which shows some loss of size of the movement in the tracking algorithm. The longitudinal movement is known to be different for individuals, and also known to be multi-phasic. By comparing the reference plot, Figure 4.10a, you can see that they do have some clear similarities in the movement pattern. Both plots start with high peaks with antegrade movement, with a following retrograde movement with a pause in the retrograde movement with a slight antegrade movement again. And then that same movement repeats. The magnitude of the movement is not the same,

which also makes these plots harder to compare. The reference image longitudinal movement shows a magnitude of around 0.8 mm in size, and the results from the 3D tracking algorithm shows only around 0.25 mm. This is a larger difference in movement size than in the radial tracking. Looking at the radial movement plot, the second slope looses shape and magnitude, however the longitudinal movement plot gains in amplitude.

Volunteer 2

For volunteer 2, the radial movement pattern looks similar, see Figures 4.6b and 4.9b, with a loss of the second slope for the 3D motion tracking. The difference in magnitude of the movement is slightly less than with volunteer 1. The 3D tracking algorithm shows a movement of around 0.35 mm, whereas the reference plot shows a movement of around 0.4 mm. Also, for the second cardiac cycle the amplitude of the radial movement drops and the shape is not as distinct. Comparing Figure 4.7b with the reference plot, Figure 4.10b, there are some distinct similarities between the two. The multi-phasic movement follows the same pattern, starting with a smaller retrograde movement, then a larger antegrade movement. The longitudinal movement plot thereafter looks a little noisy, but the retrograde movement peak at around 1 second is similar in both plots, as well as the antegrade movement peak shortly afterwards. The magnitude of these two plots also differ. The reference movement has a magnitude of around 0.3 mm, and the 3D tracking algorithm only has a magnitude of around 0.1 mm.

Volunteer 3

The 3D tracking algorithm for the radial movement for volunteer 3 has the same similarities to the reference image as the other two volunteers. Looking at Figure 4.6c, the first peak matches the reference plot, see Figure 4.9c. As with previous volunteers, the second peak fades, and even more so in this case. The magnitude of the radial movement measured with the 3D tracking algorithm was 0.35 mm, and from the reference plot the movement was around 0.6 mm. Comparing the longitudinal images it can be seen that Figure 4.7c bears a resemblance to the reference plot, Figure 4.10c. Looking at only the first cardiac cycle, until around the time of 0.9 seconds, the same basic multi-phasic movement pattern can be seen. There is an initial retrograde movement, followed by an antegrade movement, and then again retrograde movement followed by antegrade movement. The difference in magnitude is the opposite compared to the other two volunteers, with the 3D motion tracking algorithm showing a larger movement of around 0.7 mm and the reference plot shows a smaller movement of around 0.5 mm.

Similarly, for all three volunteers, the first cardiac cycle shows more accurate measurements, and then the tracking somehow ebbs away. All three radial movements were similar to each other and to the reference plots, with the magnitude of the radial movement being slightly less then the reference movement. All three longitudinal plots showed some similarities as well, although this was a lot more varied.

5.2 Sample size

When put together, the collected 3D motion images were of a very large size and there were some issues with using MATLAB together with the files. As one could guess, adding a fourth dimension will increase size massively which also increases computational time for the computer. MATLAB has a limit for how large the file size can be, which meant that some files could not be created or saved until they were downsized. Most images could be trimmed around the edges to "zoom" in on the artery to minimize file size. When sizing down the image still has to be large enough for the kernel size to match for the movement tracking, and since the artery "moved" in the images the whole set had to be considered, and even after downsizing the images were still quite large. The computational time for the movement tracking varied from around 16 hours to around 36 hours, and the resulting movement tracking files were also very large and slowed the computer down. The created move file for volunteer 3 was as large as 9.04 GB, and for the other two the files were smaller, 4,42 GB for volunteer 2 and 412 MB for volunteer 1. For further testing of this pilot study it would be recommended to use a faster computer with larger memory, as even the smallest files took a day for the movement tracking to finish. This was an issue, since MATLAB crashed often with long computation times, and the results were harder to obtain.

5.3 Acquiring data and sample quality

To collect these 4D images, 2D motion images were collected through a computerized step-motor and each step was triggered to start at the same time in the cardiac cycle using an ECG. Even though the images should have been the same throughout the cardiac cycle, each 2D motion image had a different amount of frames. To be able to make this into 3D motion images, the last frames in the larger sized 2D images were cut off. This could potentially lead to worse results, since the data wasn't always at the exact same time in the cardiac cycle.

It was very time consuming to set up for data collection. The computerized step motor moves on a straight axis and it was difficult to find a set up where the common carotid artery was in the same place in the image throughout the data sampling. The common carotid artery moved in the image which then in turn affects the movement tracking since there is an added movement in the image. This could be prevented by taking more care into the actual data collecting.

As described in the method of how the images were acquired, an ECG was used for triggering data acquisition. There are other factors in the human body which have to be considered; breathing, swallowing, use of vocal chords and pulse. Even though the ECG was used to trigger, the test subject would have to signal when he or she thought they were in the same state of breath and throat relaxation. During breathing the upper body moves to make space for air in the lungs, this movement affects the images that are acquired. Also, humans swallow and this also creates movement in the throat which affects the images. To make up for these issues, it could be possible to connect to the respiratory system and trigger on that as well as the ECG, for a complete electronically steered sample acquisition.

Also in the three different 4D images, there were a lot of darker areas. The darker areas are most often the lumen and/or structures which the ultrasounds machine has trouble detecting. This was the case in volunteer 2 and 3, the lighter area between the artery and vein was small compared to the surrounding blood, and so the movement tracking found no movement in the arterial wall. This could perhaps be resolved with the help of a block matching movement tracking combination, however due to the massive amount of computational time with just the current method of movement tracking and not enough time to apply this combination technique, no attempt at correcting with this possible method was done. In another test subject the sample quality varied in the 3D motion image. In these darker areas the movement tracking was not able to follow, since there is hardly any visible wall. This can of course be improved in the same way as the previous issues of the carotid artery moving in the collected images, by taking greater care when collecting the data.

Another way to improve the detection of the arterial wall is to use compounding on the ultrasound images. This is done by taking multiple scans of the same image, but at multiple different angles instead of just one angle. These images are then added together, this gives more visible structure of the arterial wall, since this is more easily detected from the top, and when the wall is scanned from a diagonal, other parts of the arterial wall will be more clearly visible on the ultrasound scanner. By combining all different angles of scanning, it might give better results since there is more of the arterial wall to analyze.

5.3.1 Step size

The step size for the scan of the 4D images were either 250 μm or 300 μm. This could seem quite large, since the movement, both radially and longitudinally, is is the mm range. This might affect the results with such large steps, however the distance of adjacent elements in an ultrasound transducer is around the same size. So this should not be a cause for incorrect measurements. It would be interesting to test with smaller step-size. However this would also create problems, since one main concern in this thesis is the file size of the images. With a smaller step size, more steps would be needed, the amount of depth frames would be larger and the 4D matrix would be much larger and possible too large for analysis.

5.3.2 Resolution

The resolution is lower in the z-axis direction due to the 4D image construction and the resolution in the directions of the 3D images. The step size and construction is around the same size as the placement of the adjacent piezoelectric elements and is not, as one might think, the reason for loss of resolution in the z-axis direction. The electronically steered focus point of the ultrasound in the sampled 2D images give high resolution in the axial (y-axis direction) and lateral (x-axis direction) plane. However the resolution in the elevation plane is much worse. This could affect the magnitude of the longitudinal measurement, and should not affect the magnitude of the radial measurement.

5.4 Algorithm

The movement tracking algorithm measured the movement in the x, y and z axes. As seen in all three of the volunteers segmentations, Figures 4.2, 4.3 and 4.4, the blood vessel wall is not parallel to the z-axis. The motion tracking a algorithm does not track the motion in a specific gradient, which would mean that some magnitude of the longitudinal tracking would be lost here. The same principle follows for the radial movement of the y-axis, the arterial wall is not completely parallel to any axis, and so some error in movement tracking could be derived from this.

5.4.1 Kernel size

The kernel size for movement tracking had to be chosen with some consideration of the size of the image and the size of the artery in the image. For one of the test subjects a couple of different kernel sizes were tested, to see if

the different kernel sizes affected the results. The size of the kernel affected the size of the resulting movement in both the radial and longitudinal direction. With larger kernels, the movement of the arterial wall became smaller due to more pixels standing still in the large comparison area. The size of the kernel determines the area for averaging the movement for comparison in the movement tracking algorithm. At the edges of the 3D images the movement tracking will therefor not be accurate, due to the pixels being compared to non-existent pixels outside of the image. When plotting the results the segments closest to edge were cut off, to minimize this source of error. The kernel size and sample size were connected. Since the 4D images were large in size, the need to minimize these was great. There needed to always be enough pixels around the arterial wall for the movement tracking algorithm to work, which gave the images their smallest possible size.

5.4.2 Segmentation

As one could see in 4.5, the applied movement tracking for the coordinates followed pretty well, however there were certain areas where the coordinates do not move with the arterial wall.

For volunteer 3 two different sized segmentations were made, manually, to see if the segment size had an affect on the results. One segmented shape was smaller, where the coordinates were very close or on top of the structural change from lumen to arterial wall in the ultrasound image. The other segmented shape was larger, where the coordinates were placed at a larger distance from the lumen (dark area in the image). When viewing the tracking validation for the larger segmented shape, the segmented slice looked like it followed the arterial wall more accurately than when viewing the tracking validation for the smaller segmented shape. Neither the radial nor the longitudinal movements showed any significant change however, so no further testing was done with this. None of the coordinates used in the movement tracking plots were located in the darker areas, were the movement tracking did not follow the movement as well as in other areas, so this could be a reason as to why the different sized segments did not affect the results in this thesis.

The segmentation in this thesis was done manually, and even though this was done with great care, it could be better with automatic segmentation. This could give a more accurate segmentation of the arterial wall. It could also give more possibilities for testing the movement tracking on different segmentations to see how the results vary from this. The long computational time came from the movement tracking algorithm, applying the movement to different segments took less time and was easier.

Chapter 6
Conclusion

There are a lot of things that have been considered for this thesis. This is a pilot study, and with all new areas there are a lot of unknowns, as there still is with the 3D tracking algorithm created for this thesis.

Firstly, it can be concluded that the 3D tracking algorithm shows some promise. The radial pattern follows the correct pattern more or less accurately, but with a drop in movement magnitude. The longitudinal movement shows similarities with their expected patterns and are multi-phasic, however the large loss in magnitude for the longitudinal movement and the lack of accuracy of the movement pattern shows that there is much room for improvement with this 4D tracking method. There are a few supposed reasons as why the radial and longitudinal motion magnitudes are wrong. One reason could be the amount of noise in the images. This affects the movement tracking code because the noise influences the phase difference between two frames being closer to zero than usual, and this generates a lower movement amplitude for the movement plots. The larger gradient of the linear equation will then generate a smaller movement for that pixel. This could explain the drop in magnitude for both the radial and longitudinal movement. That the longitudinal movement had an even greater drop in magnitude could maybe be explained by the movement tracking not taking into consideration the gradient of the arterial wall, and also possibly that the 4D images have a lesser resolution in the z-axis direction due to the construction of the images. A more accurate result might be gained with trying more and different kernel sizes, this was not done extensively due to the large amount of simulation time in MATLAB. Another explanation could be that the ECG signal varied, and so the amount of frames for each 2D motion image acquired (for the construction of the 4D) varied. Since the ends were cut off without any consideration other than keeping the 2D motion images of the same size, the ECG signal (and time-stamp) might vary when constructing the 4D images, creating another possible source of error. The most probable reason for the larger differences in the longitudinal

movement tracking is the resolution and sample quality in the longitudinal direction. The resolution is worse in the longitudinal direction due to the electronically steered transducer focusing in the lateral direction and having a higher lateral and axial resolution. The sample quality in the longitudinal direction is lessened due to movement of the volunteer between sampling. This movement occurs due to many reasons, one being that it is extremely hard to be completely still during image acquisitions, and the other being that there in ongoing internal movement of organs, due to blood flowing, breathing and swallowing. When the construction of the 4D images is done, the arterial wall does not line up correctly.

One main desire of this thesis was to see if there was any possibility to view a spiral motion when using 4D tracking. Due to various sources of error, this objective changed to comparing the resulting movement in the radial and longitudinal directions to reference 2D movement patterns. From the results it could be gained that 2D tracking is still the superior movement tracking method by far. Before going further with trying to gather new information using 4D movement tracking, the method of acquiring 4D images and the 3D motion tracking algorithm needs further improvement. However the results also showed it is possible to measure the longitudinal motion tracking with 4D motion tracking. The overall conclusion being that more investigating needs to be done before either ruling out this method or being able to use this 3D image tracking method.

6.1 Future work

Further work with this method is greatly needed before any real conclusion can be drawn as to whether the 3D shift phase tracking could work, and to see if it is possible to gain more knowledge of and from 3D movement of the arterial wall. The first step would be to further try and analyze the algorithm and evaluate where the drops of magnitude occur and why. Using methods to improve both the ultrasound images used, using compounding and taking samples with greater care, and more samples to compare to 2D results would be interesting. Another possible way forward would be to use an electronically controlled 3D matrix transducer to create the 4D images, and use the 3D motion tracking algorithm on those images. Yet another possible approach would be doing the motion tracking on computerized, even AI, segmentation and try to fit the motion tracking to the gradient of the slope of the arterial wall.

References

[1] World Health Organization (WHO) (2019). *Fact sheets cardiovascular diseases.* `https://www.who.int/en/news-room/fact-sheets/detail/cardiovascular-diseases-(cvds)` [2019-07-11]

[2] Persson, M., Rydén Ahlgren, Å., Jansson, T., Eriksson, A., Persson, H. W. & Lindström, K. (2003). A new non-invasive ultrasonic method for simultaneous measurements of longitudinal and radial arterial wall movements: first in vivo trial. Clinical Physiology and Functional Imaging, vol 23: pp247-251

[3] Cinthio M., Ahlgren A. R., Jansson T., Eriksson A., Persson H. W. and Lindstrom K., (2005). Evaluation of an ultrasonic echo-tracking method for measurements of arterial wall movements in two dimensions. IEEE Transactions on Ultrasonics, Ferroelectrics, and Frequency Control, vol. 52, no. 8, pp. 1300-1311.

[4] Cinthio, M., Rydén Ahlgren, Å., Bergkvist, J., Jansson, T., Persson, H. W. & Lindström, K. (2006) Longitudinal movements and resulting shear strain of the arterial wall, American Journal of Physiology-Heart and Circulatory Physiology, vol 291:H394-H402.

[5] Ahlgren, Å. R., Cinthio, M. , Steen, S. , Persson, H. W., Sjöberg, T. and Lindström, K., (2009). Effects of adrenaline on longitudinal arterial wall movements and resulting intramural shear strain: a first report. Clinical Physiology and Functional Imaging, 29: 353-359.

[6] Rydén Ahlgren, Å, Cinthio, M, Steen, S, Erlöv, T, Sjöberg, T, Persson, HW & Lindström, K (2012). Longitudinal displacement and intramural shear strain of the porcine carotid artery undergo profound changes in response to catecholamines. American Journal of Physiology: Heart and Circulatory Physiology, vol. 302, no. 5, pp. H1102-H1115.

[7] Rydén Ahlgren Å, Steen S, Segstedt S, Erlöv T, Lindström K, Sjöberg T, Persson HW, Ricci S, Tortoli P, Cinthio M, Profound Increase in Longitudinal Displacements of the Porcine Carotid Artery Wall Can Take Place Independently of Wall Shear Stress: A Continuation Report, 2015, Ultrasound in Medicine and Biology, Volume 41, Issue 5, 1342 - 1353

[8] Harloff A., Albrecht F., Stalder A. F., Bock J., Frydrychowicz A., Schöllhorn J., Hetzel A., Schumacher M., Hennig J., & Markl M. (2009). 3D Blood Flow Characteristics in the Carotid Artery Bifurcation Assessed by Flow-Sensitive 4D MRI at 3T. Magnetic Resonance in Medicine, 61:65:74.

[9] Erlöv, T., Rydén Ahlgren, Å., Albinsson, J., Segstedt, S., Nilsson, J., Jansson, T., Persson, H. W. & Cinthio, M. (2013). A fast 2D tissue motion estimator based on the phase of the intensity enables visualization of the propagation of the longitudinal movement in the carotid artery wall. IEEE–Institute of Electrical and Electronics Engineers Inc., pp. 1761-1764, IEEE International Ultrasonics Symposium (IUS), 2013, Prague, Czech Republic, 2013/07/21. https://doi.org/10.1109/ULTSYM.2013.0449

[10] Campbell, S. (2013). A short history of sonography in obstetrics and gynaecology. Facts, views & vision in ObGyn, 5(3), 213–229. PubMed PMID: 24753947; PubMed Central PMCID: PMC3987368.

[11] Martin, K. and Ramnarine, K. (2010) "Physics," in Hoskins, P. R., Martin, K., and Thrush, A. (eds) Diagnostic Ultrasound: Physics and Equipment. 2nd edn. Cambridge: Cambridge University Press, pp. 4–22. doi: 10.1017/CBO9780511750885.004.

[12] Azhari Haim (2010). Basics of biomedical ultrasound for engineers. Hoboken, New Jersey: John Wiley & Sons, Inc. pp. 313-314. doi: 10.1002/9780470561478.

[13] Martin, K. (2010) "Properties, limitations and artefacts of B-mode images," in Hoskins, P. R., Martin, K., and Thrush, A. (eds) Diagnostic Ultrasound: Physics and Equipment. 2nd edn. Cambridge: Cambridge University Press, pp. 64–74. doi: 10.1017/CBO9780511750885.007.

[14] Dudley, N. (2010) "B-mode measurements," in Hoskins, P. R., Martin, K., and Thrush, A. (eds) Diagnostic Ultrasound: Physics and Equipment. 2nd edn. Cambridge: Cambridge University Press, pp. 75–83. doi: 10.1017/CBO9780511750885.008.

[15] Erlöv, T. (2015). On the Use of Ultrasound Phase Data for Arterial Characterization. Department of Biomedical Engineering, Lund University.

[16] Martin, K. (2010) "Introduction to B-mode imaging," in Hoskins, P. R., Martin, K., and Thrush, A. (eds) Diagnostic Ultrasound: Physics and Equipment. 2nd edn. Cambridge: Cambridge University Press, pp. 1–3. doi: 10.1017/CBO9780511750885.003.

[17] Hoskins, P. and MacGillivray, T. (2010) "3D ultrasound," in Hoskins, P. R., Martin, K., and Thrush, A. (eds) Diagnostic Ultrasound: Physics and Equipment. 2nd edn. Cambridge: Cambridge University Press, pp. 171–180. doi: 10.1017/CBO9780511750885.015.

[18] Hoskins, P. (2010) "Principles of Doppler ultrasound," in Hoskins, P. R., Martin, K., and Thrush, A. (eds) Diagnostic Ultrasound: Physics and Equipment. 2nd edn. Cambridge: Cambridge University Press, pp. 84–95. doi: 10.1017/CBO9780511750885.009.

[19] Laguna, P. and Sörnmo, L. (2005) Bioelectrical Signal Processing in Cardiac and Neurological Applications. [Elektronisk resurs]. Academic Press. http://search.ebscohost.com.ludwig.lub.lu.se/login.aspx?direct=true&db=cat07147a&AN=lub.4221761&site=eds-live&scope=site [2019-06-28].

[20] Wikipedia, Anthony Atkielski, https://commons.wikimedia.org/wiki/File:SinusRhythmLabels.svg. [2019-07-09]

[21] Nichols, W. W., O'Rourke, M. F. (1998),. Properties of the arterial wall: practice. In: McDonald's Blood Flow in Arteries pp. 73–97. Edward Arnold, London.

[22] Blausen.com staff (2014). "Medical gallery of Blausen Medical 2014". WikiJournal of Medicine 1 (2). DOI:10.15347/wjm/2014.010. ISSN 2002-4436. [2019-07-12]

[23] Nichols, W. W., O'Rourke, M. F. (1998),. Ultrasonic blood flow and velocimtery. In: McDonald's Blood Flow in Arteries pp. 154–169. Edward Arnold, London.

[24] Erlöv, T., Segstedt, S., Ryden Ahlgren, A., Ricci, S., Ostling, G., Tortoli, P., Nilsson, J., Jansson, T., Persson, H. W. & Cinthio, M. (2012). A robust and fast method for arterial lumen diameter and intima-media thickness measurements. IEEE International Ultrasonics Symposium, IUS. 1678-1681. 10.1109/ULTSYM.2012.0421.

[25] Thrush, A. (2010) "Blood flow," in Hoskins, P. R., Martin, K., and Thrush, A. (eds) Diagnostic Ultrasound: Physics and Equipment. 2nd edn. Cambridge: Cambridge University Press, pp. 96–104. doi: 10.1017/CBO9780511750885.010.

[26] Soleimani, E., Dizaji, M. M., & Saberi, H. (2011). Carotid Artery Wall Motion Estimation from Consecutive Ultrasonic Images: Comparison between Block-Matching and Maximum-Gradient Algorithms. The journal of Tehran Heart Center, 6(2), 72–78.

[27] Nichols, W. W., O'Rourke, M. F. (1998),. Atherosclerosis. In: McDonald's Blood Flow in Arteries pp. 396-401. Edward Arnold, London.

[28] Nichols, W. W., O'Rourke, M. F. (1998),. Specific disease. In: McDonald's Blood Flow in Arteries pp. 402-417. Edward Arnold, London.

[29] Nichols, W. W., O'Rourke, M. F. (1998),. Hypertension. In: McDonald's Blood Flow in Arteries pp. 377-395. Edward Arnold, London.

[30] Nilsson. T., Segstedt. S., Milton. P., Sveinsdottir. S., Jansson. T., Persson. H. W., Ley. D. & Cinthio. M. (2014). Automatic measurements of diameter, distension and intima media thickness of the aorta in premature rabbit pups using B Mode images. Ultrasound Med Biol. 40(2):371 377.